



Morphological changes of mitochondria-related to apoptosis during postmortem aging of beef muscles

Chunmei Liu^{a,1}, Zhenjiang Ding^{b,1}, Zihan Zhang^a, Laiyu Zhao^a, Chunhui Zhang^a, Feng Huang^{a,*}

^a Institute of Food Science and Technology, Chinese Academy of Agricultural Sciences/Key Laboratory of Agro-Products Processing, Ministry of Agriculture and Rural Affairs, Beijing 100193, China

^b Beijing Key Laboratory of the Innovative Development of Functional Staple and Nutritional Intervention for Chronic Diseases, China National Research Institute of Food and Fermentation Industries, Beijing 100015, China

ARTICLE INFO

Keywords:

Tenderization
Mitochondrial
Outer membrane
Cristae
Fission and fusion
Apoptosis

ABSTRACT

This study aimed to investigate how postmortem muscle cells' mitochondria changed in morphology from three aspects: the outer membrane, cristae, and fission/fusion. Atomic force microscopy (AFM) results showed that mitochondria underwent a morphology transformation from normal to swelling and collapse. Meanwhile, the cleavage of OPA1, upregulation of OMA1, downregulation of Mic60 and transmission electron microscope micrographs revealed that mitochondrial cristae ruptured with an aging time extended. Additionally, the increased expressions of Fis1 and Drp1, and the AFM topographic images mutually confirmed mitochondrial fission. These results further proved from the perspective of mitochondrial morphology that the degree of mitochondrial damage increased with the postmortem aging time extended, which was consistent with the results of the release of cytochrome *c* caused by the increase of mitochondrial permeability transition pore opening and the decrease of mitochondrial membrane permeability, and further induced the apoptosis of postmortem muscle cells.

1. Introduction

The complex biochemical process of postmortem (PM) meat tenderization includes the breakdown of essential myofibrillar proteins through endogenous proteolytic enzymes (Kemp & Parr, 2012; Ding, Wei, Zhang, Zhang, & Huang, 2021). In addition to the well-studied calpains, the early PM phase sees the proteolysis of muscle proteins caused by apoptosis-causing caspases (Huang, Huang, Zhou, Xu, & Xue, 2011). It has been hypothesized that meat tenderization and PM muscle cell death were two closely linked processes (Li et al., 2022). There are three recognized apoptosis pathways in caspase-mediated apoptosis: the endoplasmic reticulum (ER) pathway, the death receptor pathway, and the intrinsic pathway (mitochondrial pathway) (Adams, 2003). When it comes to oxygen deprivation-induced PM muscle cell apoptosis, the intrinsic mitochondrial route is thought to be the primary pathway (Huang et al., 2016). Pro-apoptotic substances are released from the mitochondrial intermembrane gap during intrinsic apoptosis, which causes the mitochondrial membrane to become permeable. Amongst these intermembrane space apoptotic factors, cytochrome *c* binds Apaf-1

(the adaptor molecule apoptotic peptidase activating factor), dATP/ATP, and pro-caspase-9. As a result, this process activates the initiator caspase-9, activating executioner caspases (Green, 2005).

For a long time, the three most frequently employed indicators to describe the level of mitochondrial damage in the process of PM meat tenderization are mitochondrial membrane permeability (MMP), mitochondrial permeability transition pore (MPTP) opening, and mitochondrial ultrastructure by transmission electron microscope (TEM). Mitochondria have a typical lipid bilayer membrane structure, including outer membrane and inner membrane (Quintana-Cabrera, Mehrotra, Rigoni, & Soriano, 2018). Folds into the mitochondrial matrix to form concave structures of varying sizes and shapes called cristae and the junction between the inner boundary membrane and cristae is a narrow neck-like structure called cristae junction (Mukherjee, Ghosh, & Meinelcke, 2021). Some scholars believe that 85% of cytochrome *c* is found to exist in the mitochondrial cristae structure. Suppose the outer membrane permeability directly releases cytochrome *c*. In that case, it should be free to pass through the cristae structure, and a large amount of cytochrome *c* cannot be stably stored in the cristae structure (Quintana-

* Corresponding author at: No. 1, Nongda South Rd., Xi Beiwang, Haidian District, Beijing 100193, China.

E-mail address: fhuang226@163.com (F. Huang).

¹ Both authors contributed equally to the work.

Cabrera et al., 2018). It has been proposed that cytochrome c release during apoptosis can be divided into a two-step process, beginning with the protein's separation from the inner membrane under the control of mitochondrial ultrastructure, then causing the outer membrane to become permeable and cytochrome c to be released into the cytoplasm (Gogvadze, Orrenius, & Zhivotovsky, 2006). Existing studies have focused on mitochondrial apoptosis caused by outer membrane permeability and MPTP channel openness (Wang et al., 2018). However, there are few studies on mitochondrial inner membrane cristae structure in PM skeletal muscles. Our previous reports have demonstrated that Mic60, Mic19, and Mic27, which regulate cristae morphology and the growth of mitochondrial contact sites, showed a considerable decrease in expression at 24 h PM (Liu et al., 2022). However, how the inner mitochondria's morphological control and cristae production work is still unknown. Therefore, the purpose of this study was to break through the previous evaluation indicators of mitochondrial damage, investigate the changes in the outer membrane and cristae structure, as well as the expression of fission or fusion factors during PM mitochondrial apoptosis of beef muscles, to characterize the possible mechanism of mitochondrial ultrastructure in regulating the apoptosis of PM beef muscle cells from a multidimensional perspective.

2. Materials and methods

2.1. Experimental design

Six head of 3-year-old Chinese yellow cattle (average live weight: 584.6 kg) were slaughtered at a commercial meat processing company (Hebei Fucheng Wufeng Food Co. LTD), as required by the National Standard "Operation Rules for Beef Cattle Slaughter of the People's Republic of China". The protocol was approved by the Animal Care and Ethics Committee of Chinese Academy of Agricultural Sciences (IAS20160616; date: 2016, Beijing, China). Within 30 min, six *Longissimus thoracic* (LT) muscles from six cows were extracted from the carcasses. Each LT muscle was taken and removed from the fascia and connective tissues and cut into 10 pieces, 20 g each, wrapped with tin foil, and immediately put into liquid nitrogen as 0 h PM samples. Three groups of six LT muscle components were created at random. Each group was individually aged at 4 °C for 6, 24, 72, and 120 h, respectively, then collected at the corresponding time points to prepare transmission electron microscopy and apoptosis samples. Then three groups of muscle samples were collected and frozen in the -80 °C refrigerator to determine the biochemical indexes.

2.2. Isolation of subcellular components

The method described by Wang et al. (2018) was followed with a few minor modifications for the isolation of subcellular components. Ten times the volume of precooled extraction buffer was used to homogenize 5 g of sliced muscle. The mixture was spun at 1000 g and 4 °C for 10 min by a centrifuge. A second centrifugation under the same circumstances was performed on the acquired supernatant. The mitochondria and cytoplasm were then obtained by centrifuging the supernatant at 8000 g for 20 min at 4 °C. The precipitate after centrifugation were mitochondria, and the supernatant were cytosolic-enriched proteins. A suspension of the resulting mitochondrial pellets was made in the top extraction buffer. The protein concentration was calculated by a BCA Protein Assay kit.

2.3. Caspases activity assays

The Caspase fluorescence assay kit (Biovision, USA) was used to measure the activities of caspase-3 and caspase-9. The shredded muscle (1 g) was placed in lysis buffer (3 mL) and lysed at 15,000 rpm 3 times, 10 s apart, using a Polytron homogenizer (IKA, Germany). The tissue lysate was then centrifuged at 4 °C and 16,000 g for 15 min to obtain the

supernatant. The protein concentration adjusted to 5 mg/mL. The soluble fraction was collected, and 50 μ L $2 \times$ Reaction buffer was added, then 5 μ L DEVD-AFC and LEHD AFC substrate (final concentration 50 μ M) were added, respectively. After that, the mixture was incubated for 2 h at 37 °C. Fluorescence values were measured in a SynergyH1M (BioTek, USA) with a 400 nm excitation filter and a 505 nm emission filter.

2.4. Apoptotic nuclei assays

Apoptotic cell DNA fragments were detected by terminal deoxynucleotidyl transferase (TdT) mediated dUTP gap terminal marker (TUNEL). The sample was cut into $1.0 \times 0.5 \times 0.5$ cm³ slices, then fixed, embedded, sliced, and sealed. After rinsing 3 times in PBS buffer, 100 μ L protease K working solution was added to each sample and reacted at 37 °C for 30 min, then rinsed with PBS buffer 3 times again. The sections were dried with absorbent paper, and each section was added with 50 μ L TdT enzyme solution and reacted at 37 °C for 1 h. After the reaction, the sample portion was immersed in a PBS buffer solution and rinsed 3 times away from light. Sections were placed in Streptavidin-FITC labeled solution and reacted for 30 min. Diaminobenzidine (DAB) was dyed for 10 min without light. Finally, the PBS buffer solution was washed 3 times under dark conditions, and a fluorescence microscope was used to observe and count.

2.5. Detection of MPTP opening

Referring to Hu et al. (2015) method with slight modification, mitochondrial particles were suspended in a cooled MPTP medium, and the protein concentration of the mixture was adjusted to 1 mg/mL. 50 μ L of the purified mitochondrial particle suspension (1 mg/mL) and 150 μ L cooled MPTP test medium was added to a 96-well plate. A microplate reader (BioTek, USA) measured the absorbance at 540 nm.

2.6. Detection of MMP

The JC-1 assay reagent (Solarbio, Beijing, China) was utilized to measure MMP. The JC-1 staining working solution was incubated with the pure mitochondrial solution for 20 min. The detection bands for JC-1 monomers and aggregates were 490/530 nm and 525/590 nm, respectively.

2.7. Atomic force microscopy observation

The previously described procedure was used with a few minor modifications (Lee et al., 2011). The amount of mitochondrial protein was raised to 2 mg/mL using an adsorption buffer. Onto a spotless bit of mica, the mitochondrial solution was poured. After a short period of air drying at room temperature, the prepared samples were immediately imaged by an atomic force microscope (Park NX10, Korea).

2.8. Mitochondrial micromorphology detection

Using a slightly modified version of Grogan et al. (2002) methodology, beef muscles were cut at 0, 6, 24, 72, and 120 h after slaughter. All muscle strips were cut into $1 \times 1 \times 3$ mm³ slices, solidified in 0.1 M phosphate buffer with 3% glutaraldehyde, and then placed in 2% osmium tetroxide for secondary fixation. To place the sample into Epon812 resin and cut it with Power TOM-XL, it was first dehydrated in ethanol. Lead citrate and uranium acetate were used to stain ultrathin slices. Transmission electron microscopy was used to examine the muscle (Hitachi H-750, Japan).

2.9. Whole muscle protein preparation

The whole muscle protein was extracted as previously reported

(Zhang, Ma, & Kim, 2020) with a few small modifications. The minced muscle was homogenized in extraction buffer that had been previously cooled, and it was then centrifuged at 20,000 g. The BCA Protein Assay kit was used to assess the concentration of protein.

2.10. SDS-PAGE and western blotting

All SDS-PAGE samples were thoroughly combined with the sampling treatment buffer. The expression level of Fis1 and Cyt-c were detected by

15% gels, the expression level of Drp 1, Mic60, OMA1 and OPA1 were detected by 12.5% gels. The gels underwent 3 h of 120 V electrophoresis on the Bio-Rad Mini-Protein II equipment. The target proteins were transferred for 90 min at 200 mA at 4 °C onto polyvinylidene fluoride membranes. Membranes were blocked with 5% (w/v) nonfat dry milk in Tris-buffered saline at room temperature for 2 h. The membrane was then incubated at 4 °C for 14 h with anti-cytochrome C (ab110325, abcam), anti-OPA1 (ab157457, abcam), anti-OMA1 (ab154939, abcam), anti-Drp1 (ab184247, abcam), anti-Fis1 (ab156856, abcam) and anti-

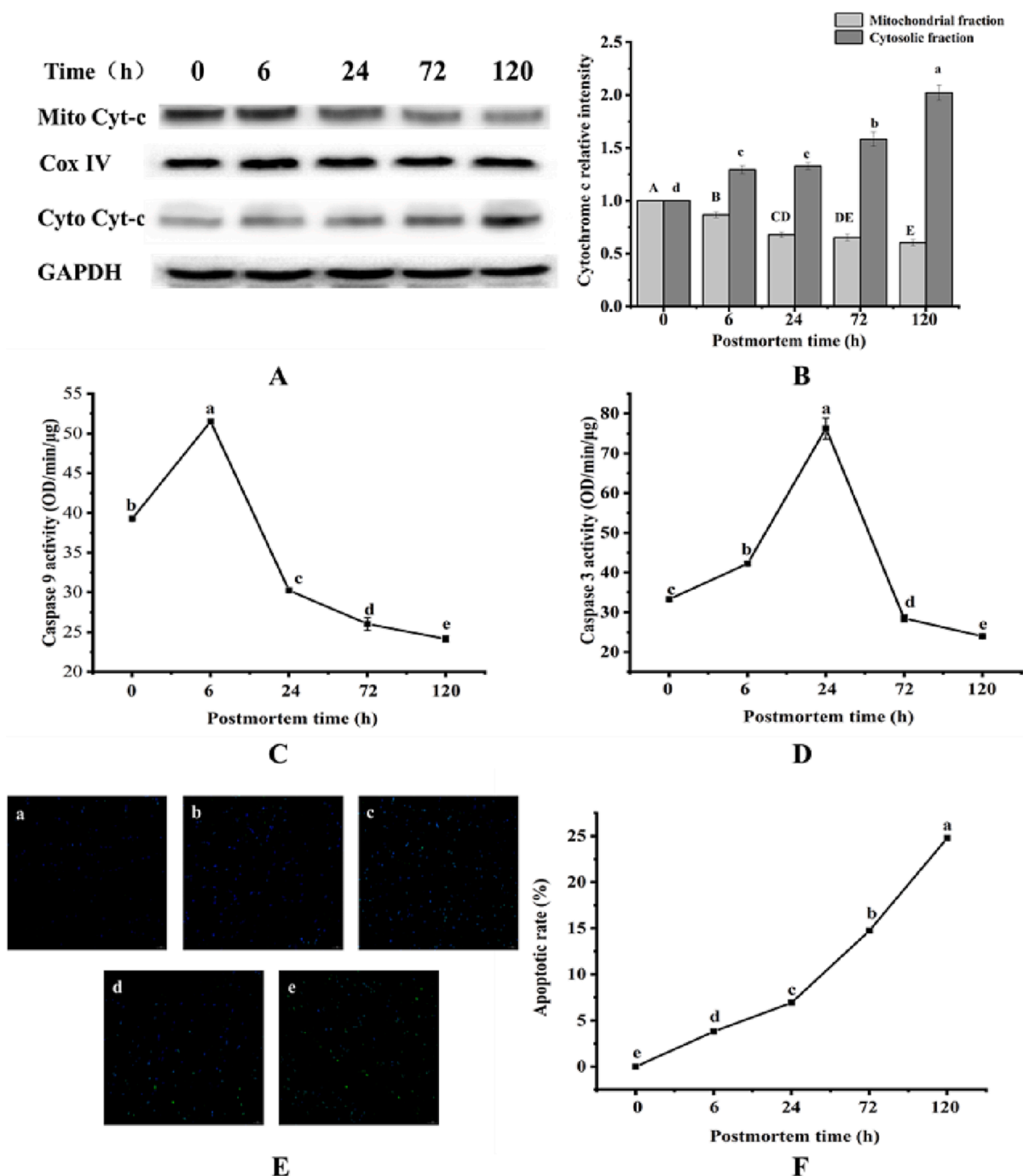


Fig. 1. The changes of cytochrome *c* release, caspases activities and apoptosis rate in postmortem beef muscles. (A) The expressions of cytochrome *c* in mitochondria and cytoplasm fractions in bovine muscle during postmortem aging. Densitometric analysis of cytochrome *c* was shown in (B). Changes caspase-9 activity (C) and caspase-3 activity (D) in bovine muscle during postmortem aging. (E) Representative TUNEL photographs of apoptotic nuclei ($\times 400$) in bovine muscle during postmortem aging, normal nuclei were labeled with blue fluorescence by adopting 4',6-diamidino-2-phenylindole (DAPI) dyes, whereas the apoptotic nuclei were labeled with green fluorescence through TUNEL. (F) The apoptotic rate was obtained by the ratio of TUNEL and DAPI. Data are presented as mean \pm SD ($n = 3$). Different letters (a-e, A-E) are significant difference ($p < 0.05$).

Mic60 (Q16891, abmart), The membranes were then treated with secondary antibodies that were conjugated to HRP-conjugated secondary antibodies (A9044, Sigma, USA) for 2 h after being rinsed four times in TBS. The membranes were then scanned using a Chemi-Doc TMMP Imaging System (Bio-Rad) and the densities of protein bands were examined using Image J software after four more washes.

2.11. Warner-Bratzler shear force

Tenderness was evaluated by Warner-Bratzler shear force (WBSF) which was measured as described before (D'Alessandro, Marrocco, Zolla, D'Andrea, & Zolla, 2012b). The muscle samples were cut into pieces (1 cm² cross section) parallel to the orientation of muscle fiber before cooked in a 72 °C water bath until internal temperature reached 70 °C. After being cooled to room temperature the cooked sample was sheared using a stable Micro System Texture Analyzer (Stable Micro System Ltd. Godalming, UK) equipped with a WBSF device.

2.12. Statistical analysis

Atomic force 3D morphology was analyzed by XEI and Gwyddion software. The data of apoptosis rate, caspase activities, mitochondrial membrane potential, MPTP, WBSF, and mitochondrial external morphology were conducted by SPSS 25.0 software by one-way ANOVA in conjunction with Duncan's New Multiple-range test. Data were expressed as mean ± SD (n = 3). Statistical significance was identified as *p* value < 0.05.

3. Results and discussion

3.1. Cytochrome *c* release, caspase-9/3 activities and apoptotic nuclei

In mammalian cells, mitochondria serve as a site of convergence for a variety of cell death signals, and they have traditionally been regarded as the sentencers and executors of cell death sentences (Bhola & Letai, 2016). The primary mechanism of apoptosis in the mitochondrial route was the release of apoptotic agents like cytochrome *c* in mitochondria (Jiang et al., 2019). Cytochrome *c* in mitochondria was first examined whether it was released into the cytoplasm in PM beef muscles by accessing the expression level of cytochrome *c* in the cytosolic fraction and the mitochondrial fraction, respectively (Fig. 1A). With the aging time extended, notably at 6–24 h PM, the quantity of cytochrome *c* in the mitochondrial fraction drastically fell (*p* < 0.05). On the other hand, for the first 6 h PM, the level of cytochrome *c* in the cytosolic fraction dramatically rose (*p* < 0.05) (Fig. 1B). These results have also been found in previous reports (Huang et al., 2016), which possibly resulted from the mitochondrial cytochrome *c* was synthesized more quickly than it was released. Another possible explanation is that cytochrome *c* was temporarily redirected from the cytoplasm to the mitochondria as a result of cell self-defense. In PM beef muscle, cytochrome *c* is primarily released from mitochondria to the cytoplasm. These results validated past research using equivalent methods that demonstrated early PM cytochrome *c* release from mitochondria to cytoplasm. (Huang et al., 2016; Wang, Han, Ma, Yu, & Zhao, 2017).

Apoptosomes were formed when procaspase-9 and the apoptotic protease activating factor-1 (Apaf-1) coupled to the released cytochrome *c*, caspase-3 was then activated (Ding et al., 2021). With the highest activity for caspase-9 and caspase-3 at 6 h and 24 h, respectively, the activities of caspase-9 and caspase-3 first increased and then declined (Fig. 1C,D). These findings were in line with those of Wang et al. (2017), who also discovered that procaspase-9 was activated before procaspase-3. Additionally, the detection of apoptotic nuclei in aged bovine muscle was shown in Fig. 1E. The apoptotic nuclei were largely undetectable for the first 6 h PM. However, the number gradually increased as the aging period lengthened, and the apoptosis rate of cells increased to 24.78% at 120 h (Fig. 5F). This matched the findings of Zhang et al. (2018). The

above results suggested that the mitochondrial-mediated release of apoptotic factors is a key pathway for regulating the apoptosis of PM beef muscle cells.

3.2. MPTP opening and MMP

According to Liu et al. (2012), the opening of MPTP has been identified as the primary pathway for mitochondrial cytochrome *c* release. Furthermore, the depolarization of MMP occurred concurrently with the release (Wang et al., 2017). So, the openness of MPTP and MMP of isolated mitochondria from PM beef muscles were examined in the present study. Absorbance changes are generally used to access MPTP openness, and absorbance decline reflects increased MPTP openness. Fig. 2A showed that MPTP openness increased significantly (*p* < 0.05) from 0 h to 120 h. On the other hand, as shown in Fig. 2B, the MMP decreases significantly (*p* < 0.05) with the aging time extended. These results were consistent with several earlier investigations conducted by researchers (Wang et al., 2017; Zhang et al., 2020), who discovered the initiation of MPTP and the decrease of MMP throughout PM aging. These results supported that the openness of MPTP and MMP of isolated mitochondria from PM beef muscles were recognized to assess mitochondrial damage.

3.3. Outer membrane structure of mitochondria

The outer membrane and inner membrane are two typical lipid membrane structures of mitochondria. The outer membrane is involved in a variety of biological processes and is closely linked to mitochondrial morphology, including swelling and condensation. One of the most significant indicators of MPTP opening is swelling caused by the mitochondrial outer membrane, which is generally acknowledged (Lee et al., 2011). Although mitochondrial swelling has been examined by measuring light scatter or fluorescence microscopic observations, quantitative analysis of them by use of atomic force microscopy (AFM), with the advantages of high-resolution microscopic bio-imaging without rigorous and complex operation, has been widely employed as a morphological analysis tool for mitochondrial outer membrane (Gao et al., 2017; Lee et al., 2013). However, there was less attention focused on immediate changes of mitochondria in PM apoptotic cells. We first characterized the outer membrane morphology changes in mitochondria from PM beef skeletal muscles in the present study. As shown in AFM three-dimensional images (Fig. 3), with the aging time extended, the mitochondria undergo the transformation process of morphological change from normal to swelling and collapse. At 0 h after slaughter, the surfaces of mitochondria were observed to be relatively smooth and integrated. At 6 h PM, the mitochondria were swollen and expanded with a smooth surface. At 24 h PM, the mitochondria started to collapse from the center and its surface became rugged. At 72 h PM, the mitochondria had an irregular collapse and increasing surface roughness, with rugged texture in the center and further enlarged diameter. Intact mitochondria morphology could not be observed at 120 h PM. The swelling phenomenon based on AFM was similar to the results from ischemic heart mitochondria (Lee et al., 2011) and Parkinson's brain mitochondria (Lee et al., 2017). However, the collapse of mitochondria in our study was not observed in the above two reports, which was possibly induced by the extreme apoptosis and even by the other types of cell death in PM muscle cells. After all, skeletal muscle cells are multinucleated and their death of them may exhibit multiple types, namely, apoptosis, autophagy, and even necroptosis (Adhichetty & Hood, 2003) because wholesale myofiber cell death has a lower frequency of occurrence than individual myonuclear decay.

To further characterize the morphological changes in the mitochondrial outer membrane from PM beef muscle cells, the particle analysis module was utilized to identify and quantify mitochondria. As shown in Table 1, with the increase in aging time, the maximum mitochondrial length, width, and roughness increased significantly (*p* <

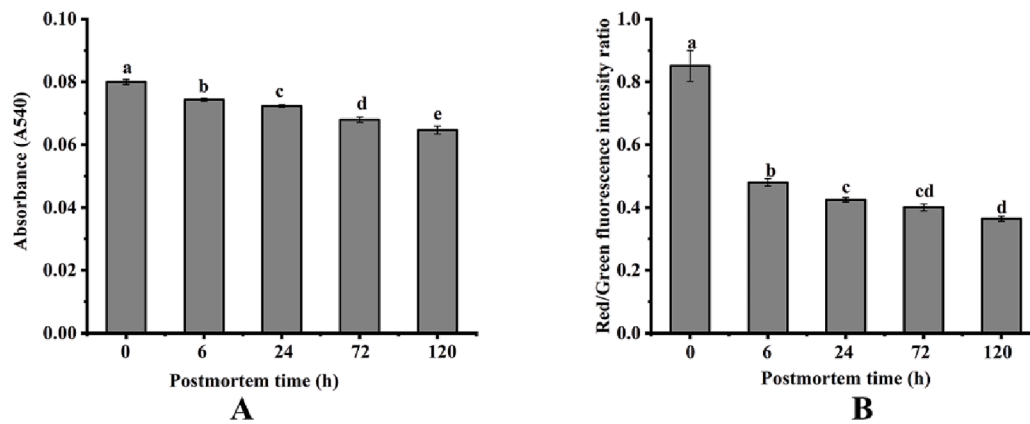


Fig. 2. The changes of MPTP opening (A) and mitochondrial membrane potential (B) in bovine muscle during postmortem aging. Data are presented as mean \pm SD (n = 3). Different letters (a-e) are significant difference ($p < 0.05$).

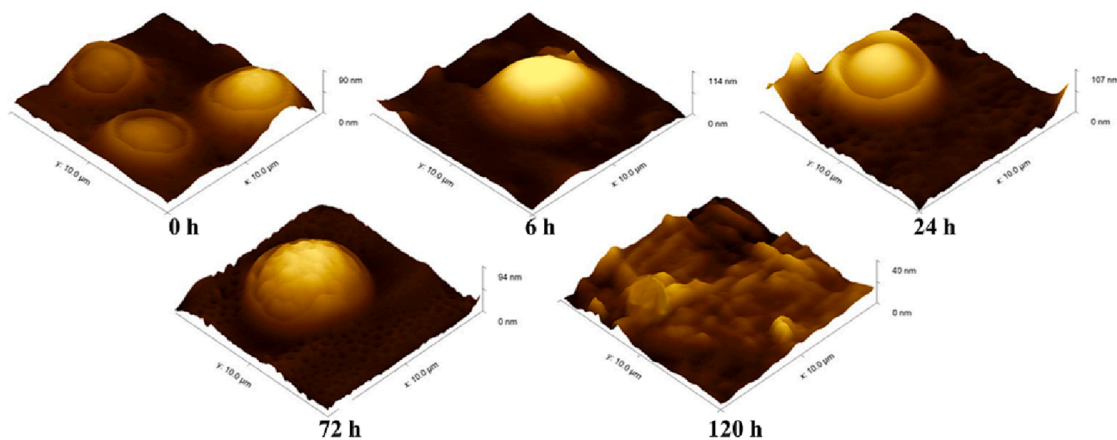


Fig. 3. The changes of outer membrane structure of mitochondria. Representative AFM 3D topographic images of mitochondria in bovine muscle during postmortem aging, scale bars represent $10 \mu\text{m} \times 10 \mu\text{m}$.

Table 1

Shape analysis parameters for the ultrastructural changes during postmortem beef aging.

Postmortem time/h	Length/ μm	Width/ μm	Maximum Height/nm	Average Roughness/nm
0	4.87 \pm 0.18 ^c	3.82 \pm 0.04 ^c	90 ^c	10.34 \pm 0.68 ^d
6	5.82 \pm 0.08 ^b	3.85 \pm 0.07 ^c	114 ^a	19.77 \pm 0.13 ^c
24	5.90 \pm 0.07 ^b	4.52 \pm 0.06 ^b	107 ^b	19.39 \pm 1.19 ^c
72	7.38 \pm 0.16 ^a	5.53 \pm 0.09 ^a	94 ^c	23.05 \pm 0.17 ^b
120	/	/	40 ^d	49.17 \pm 0.28 ^a

Predicted means \pm standard error for mitochondria length, width, maximum height, and average roughness. Data are presented as mean \pm SD (n = 3). Different letters (a-d) in the same column indicate a significant difference between aging time ($p < 0.05$).

0.05), and mitochondrial highness increased at 0–6 h PM, with little changes between 6 h and 24 h PM, and subsequently fell from 24 h to 120 h PM. AFM-based ultrastructural study of the mitochondria revealed that the size of the mitochondria significantly increased during PM aging in beef muscle. According to previous findings, alterations in four metrics, including mitochondrial length, width, height, and roughness, may be a reflection of morphological variations (Lee et al., 2013). Therefore, the results of nanostructure by AFM and its quantitative analysis

provided direct supporting evidence for swelling regulated by the mitochondrial outer membrane in PM beef muscle cells, breaking through the mitochondrial damage reflected by conventional MPTP openness and MMP.

3.4. Cristae structure of mitochondria in PM beef muscles

The mitochondrial inner membrane folds into the matrix to form a concave structure with different sizes and shapes called cristae. The junction between the inner boundary membrane and the ridge is a narrow neck-like structure called the cristae junction. The reconstruction of mitochondrial cristae (cristae morphological change, cristae junction expansion, etc.) to open the channels inside the cristae is recently considered a required step for the complete release of cytochrome c (Ulivieri, 2010). For analyzing the changes in ultrastructure connected to the release of proteins, transmission electron microscopy (TEM) with better resolution is a useful tool (Sun et al., 2007). TEM observation was performed on in situ muscle slices at 0, 6, 24, 72, and 120 h PM to further investigate the internal morphological changes of mitochondria during PM aging. As shown in Fig. 4A, mitochondrial morphology changed significantly with the aging time extended. At 0 h PM, the mitochondrial structure was intact and similar to that of physiological mitochondria, with a smooth outer membrane, compact cristae structure, and clear fold arrangement. At 6 h PM, the size of mitochondria had a visible increase. The outer membrane was still intact while the number of mitochondrial cristae decreased apparently. At 24 h PM, mitochondrial size increased ulteriorly, and meanwhile, the

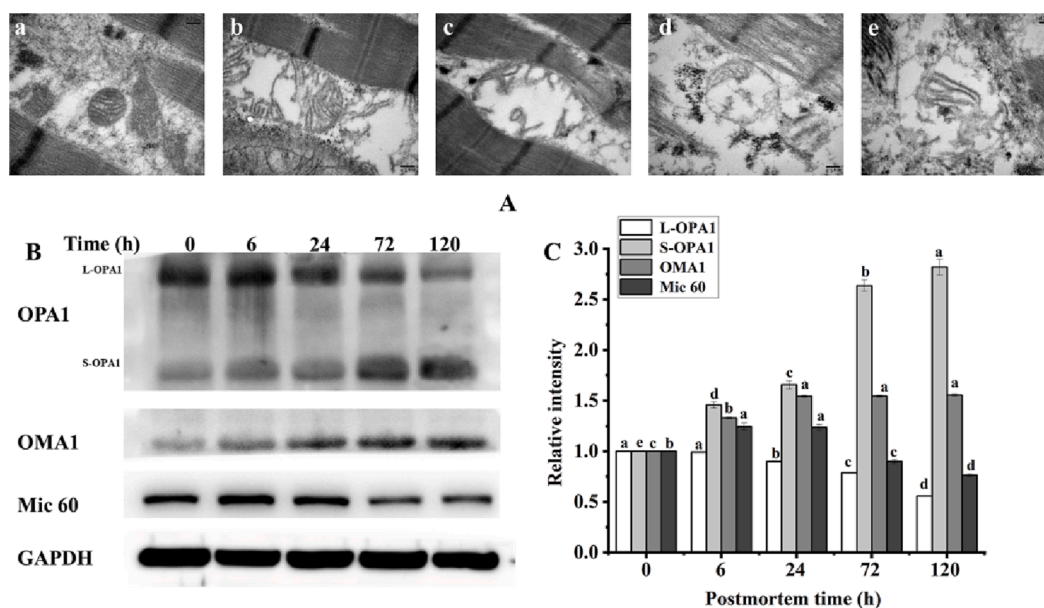


Fig. 4. The changes of cristae structure of mitochondria. (A) TEM images of the internal ultrastructure of mitochondria during postmortem aging. (B) The expressions of L-OPA1, S-OPA1, OMA1, and Mic60 in bovine muscle during postmortem aging. Densitometric analysis of them were shown in (C). Data are presented as mean \pm SD ($n = 3$). Different letters (a-e) are significant difference ($p < 0.05$).

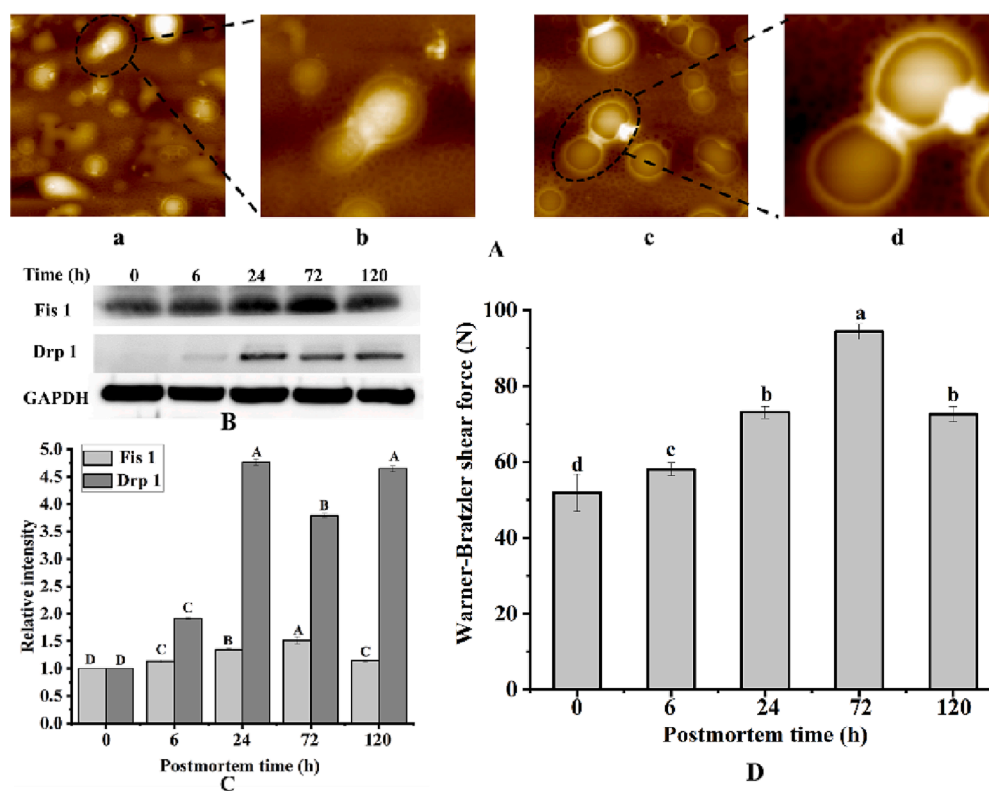


Fig. 5. The changes of fission/fusion of mitochondria. (A) Representative AFM 2D topographic images of mitochondria at 0 and 24 h postmortem, scale bars represent $10 \mu\text{m} \times 10 \mu\text{m}$ (a, c) and $25 \mu\text{m} \times 25 \mu\text{m}$ (b, d), respectively. (B) The expressions of Fis1 and Drp1 in bovine muscle during postmortem aging. Densitometric analysis of them were shown in (C). (D) The Warner-Bratzler shear force of *Longissimus thoracic* muscles during postmortem aging. Data are presented as mean \pm SD ($n = 3$). Different letters (A-D) are significant difference ($p < 0.05$).

mitochondrial outer membrane started to be ruptured. The length of mitochondria was shortened and some of the mitochondria exhibited the vesicular ultrastructure. At 72 h PM, the mitochondrial membrane structure was seriously ruptured, and the size decreased. Moreover, mitochondrial cristae structure also became vague. At 120 h PM, mitochondria were fragmented apparently and only some cristae fragments could be observed.

According to mounting evidence, the protein complex containing the

fusion protein OPA1 was responsible for locking the majority of cytochrome c inside cristae and was essential for the remodeling of cristae. OPA1 has a long-form (L-OPA1) and a short form (S-OPA1), and it is found in the intermembrane space. It controls the size of the cristae junction and the fusion of the inner mitochondrial membrane. Generally, L-OPA1 kept junctions narrow, whereas S-OPA1 widened the junctions (Bock & Tait, 2020). So, we subsequently examined the changes of OPA1 in PM beef muscles. As shown in Fig. 4B and C, with an

increasing aging time, the expression level of L-OPA1 significantly ($p < 0.05$), whereas that of S-OPA1 increased significantly ($p < 0.05$). These results demonstrated that L-OPA1 could be cleaved into S-OPA1 in PM beef muscles, which has been revealed in many types of apoptotic cells (Jiang, Jiang, Shen, & Wang, 2014). Given the critical roles of L-OPA1 in stabilizing the cristae, proteolysis of L-OPA1 into S-OPA1 was helpful to mitochondrial cristae remodeling and fragmentation. To further investigate the reason for L-OPA1 proteolysis, we examined the expression level of mitochondrial metalloprotease OMA1 in PM beef muscles, which was responsible for cleaving L-OPA1, leading to oligomer disassembly and junction opening (Bock & Tait, 2020). With the extension of the aging period, the expression level of OMA1 considerably increased ($p < 0.05$), which agreed with the changes in OPA1 expression. These results highlighted the important role of OMA1 and OPA1 in characterizing the integrity of mitochondrial cristae in PM beef muscle.

Recently, several laboratories had identified a new complex MICOS, mainly located at the mitochondrial cristae junction point (CJs) and responsible for regulating cristae morphology and the formation of cristae (Jans et al., 2013). A vital component of the MICOS complex, Mic60 was essential for maintaining the shape of the mitochondrial cristae (Harner et al., 2011). Mic60 interacted with several protein complexes in the outer mitochondrial membrane, which are strongly associated with mitochondrial apoptosis, in addition to taking a role in the regulation of cristae and cristae junction formation (Ikeda et al., 2020). In the current study, Mic60 expression increased at 0–6 h PM and then dramatically declined at 24–120 h (Fig. 4B, C). The increase of Mic60 at 0–6 h PM possibly resulted from the cell self-protection to maintain mitochondrial regular structure. However, after exsanguination and bleeding of animals, extreme environmental conditions soon break these self-protective systems, which induced the decrease of Mic60. These results were also by the destruction of mitochondrial cristae structures.

3.5. Fission or fusion of mitochondria and WBSF of PM beef muscles

Mitochondrial fission/fusion was characteristic of the intrinsic apoptosis pathway. Interestingly, we observed the phenomenon of two mitochondria adhering together on AFM topographic images of 0 h and 24 h PM (Fig. 5A), which was not observed at 72 h and 120 h PM. The mitochondrial adhesion rarely occurs between 0 and 6 h after slaughter, while it frequently occurs after 24 h of slaughter. The two attached mitochondria also had different degrees of adhesion, some of which were initially touched, and another was seemingly wholly merging. Meanwhile, the lightness at the adhering edge increased apparently, which means an increasing highness. Unfortunately, it was not sure whether this represents the fission or fusion of mitochondria merely based on the AFM topographic images.

In addition to fusion, increased fission appeared to be a prerequisite for cytochrome *c* release (Pernas & Scorrano, 2016). One of the most significant fission proteins, Drp1, has been suggested to help in cytochrome *c* release and could promote cristae (Bock & Tait, 2020). The expression of Drp1 increased significantly with the aging time extended, and especially at 24 h PM (Fig. 5B, C), which was by the appearance of mitochondrial fission on AFM topographic images. Drp1 was recruited to the mitochondrial surface to start the intricate process of mitochondrial fission. It has been hypothesized that Drp1 was moved to potential mitochondrial fission sites via Fis1 (Pernas & Scorrano, 2016). So, we also examined the changes in Fis1 content in PM muscle cells and found that the expression of Fis1 increased with the aging time extended, and the increase of Fis1 occurred earlier than that of Drp1 (Fig. 5B, C). These results support the expression levels of Drp1 and Fis1 as indicators for evaluating mitochondrial damage mediated by fission/fusion.

WBSF is one of the key indicators for evaluating meat tenderness. In order to further explore the intrinsic relationship between mitochondrial damage and tenderness during postmortem aging, WBSF was measured and the result was shown in Fig. 5D. The WBSF increased first

and then decreased, and reached the maximum at 72 h after slaughter, which was considered to reached rigor mortis levels, consistent with Wang's study (Wang et al., 2018). Compared with the WBSF at 72 h, the decrease of WBSF at 120 h may be closely related to Fis1 mediated mitochondrial fission and blurred contour of mitochondrial cristae structure at 120 h. These results indicated a certain correlation between mitochondrial damage and tenderness. Additionally, the conclusion of this study needs to be further validated in subsequent research models on mitochondrial damage regulators. The next research will focus on constructing specific research models to elucidate the mechanism of different mitochondrial damage regulatory factors on PM meat tenderness.

4. Conclusions

In summary, The increase of cytochrome *c* release, the activation of caspase-9/3, the increase of MPTP opening and the decrease of MMP were the basic evaluation indicators used in this investigation to show that PM beef muscles had suffered mitochondrial damage. Additionally, the transition from normal to swelling and collapse in the morphology of the mitochondrial outer membrane, blurred contour of mitochondrial cristae structure, and imbalance of mitochondrial fission/fusion as aging progressed were revealed through morphological research and changes of key proteins expressions. Therefore, this study revealed the changing rules of mitochondrial damage in PM beef muscle cells from three aspects: mitochondrial outer membrane, cristae, and fission/fusion.

CRedit authorship contribution statement

Chunmei Liu: Conceptualization, Investigation, Methodology, Data curation, Validation, Visualization, Writing – original draft. **Zhenjiang Ding:** Conceptualization, Data curation, Visualization, Writing – review & editing. **Zihan Zhang:** Methodology, Software, Data curation, Writing – review & editing. **Laiyu Zhao:** Data curation, Supervision. **Chunhui Zhang:** Conceptualization, Project administration, Supervision. **Feng Huang:** Conceptualization, Methodology, Supervision, Writing – review & editing, Funding acquisition.

Declaration of Competing Interest

The authors declare that they have no known competing financial interests or personal relationships that could have appeared to influence the work reported in this paper.

Data availability

No data was used for the research described in the article.

Acknowledgments

This work was supported by the National Natural Science Foundation of China (Grant Nos: 32072244).

References

- Adams, J. M. (2003). Ways of dying: Multiple pathways to apoptosis. *Genes & Development*, 17(20), 2481–2495.
- Adhithetty, P., & Hood, D. (2003). Plasticity of skeletal muscle mitochondria in response to contractile activity. *Experimental Physiology*, 88(1), 99–107.
- Bhola, P. D., & Letai, A. (2016). Mitochondria—Judges and Executioners of Cell Death Sentences. *Molecular Cell*, 61(5), 695–704.
- Bock, F. J., & Tait, S. W. G. (2020). Mitochondria as multifaceted regulators of cell death. *Nature Reviews Molecular Cell Biology*, 21(2), 85–100.
- Ding, Z. J., Wei, Q. C., Zhang, C. H., Zhang, H., & Huang, F. (2021). Influence of oxidation on heat shock protein 27 translocation, caspase-3 and calpain activities and myofibrils degradation in postmortem beef muscles. *Food Chemistry*, 340, Article 127914.
- Gao, G., Wang, Z., Lu, L., Duan, C., Wang, X., & Yang, H. (2017). Morphological analysis of mitochondria for evaluating the toxicity of α -synuclein in transgenic mice and

- isolated preparations by atomic force microscopy. *Biomedicine & Pharmacotherapy*, 96, 1380–1388.
- Gogvadze, V., Orrenius, S., & Zhivotovsky, B. (2006). Multiple pathways of cytochrome c release from mitochondria in apoptosis. *Biochimica et Biophysica Acta (BBA) - Bioenergetics*, 1757(5), 639–647.
- Green, D. R. (2005). Apoptotic Pathways: Ten Minutes to Dead. *Cell*, 121(5), 671–674.
- Grogan, S. P., Aklin, B., Frenz, M., Brunner, T., Schaffner, T., & Mainil-Varlet, P. (2002). In vitro model for the study of necrosis and apoptosis in native cartilage. *The Journal of Pathology*, 198(1), 5–13.
- Harner, M., Korner, C., Walther, D., Mokranjac, D., Kaesmacher, J., Welsch, U., ... Neupert, W. (2011). The mitochondrial contact site complex, a determinant of mitochondrial architecture. *The EMBO Journal*, 30(21), 4356–4370.
- Hu, Y., Yan, J. B., Zheng, M. Z., Song, X. H., Wang, L. L., Shen, Y. L., & Chen, Y. Y. (2015). Mitochondrial aldehyde dehydrogenase activity protects against lipopolysaccharide-induced cardiac dysfunction in rats. *Molecular Medicine Reports*, 11(2), 1509–1515.
- Huang, F., Huang, M., Zhang, H., Zhang, C. J., Zhang, D. Q., & Zhou, G. H. (2016). Changes in apoptotic factors and caspase activation pathways during the postmortem aging of beef muscle. *Food Chemistry*, 190, 110–114.
- Huang, F., Huang, M., Zhou, G. H., Xu, X. L., & Xue, M. (2011). In Vitro Proteolysis of Myofibrillar Proteins from Beef Skeletal Muscle by Caspase-3 and Caspase-6. *Journal of Agricultural and Food Chemistry*, 59(17), 9658–9663.
- Ikeda, H., Muroi, M., Kondoh, Y., Ishikawa, S., Kakeya, H., Osada, H., & Imoto, M. (2020). Miclxin, a Novel MIC60 Inhibitor, Induces Apoptosis via Mitochondrial Stress in beta-Catenin Mutant Tumor Cells. *ACS Chemical Biology*, 15(8), 2195–2204.
- Jans, D. C., Wurm, C. A., Riedel, D., Wenzel, D., Stagge, F., Deckers, M., ... Jakobs, S. (2013). STED super-resolution microscopy reveals an array of MINOS clusters along human mitochondria. *Proceedings of the National Academy of Sciences of the United States of America*, 110(22), 8936–8941.
- Jiang, X., Jiang, H., Shen, Z. R., & Wang, X. D. (2014). Activation of mitochondrial protease OMA1 by Bax and Bak promotes cytochrome c release during apoptosis. *Proceedings of the National Academy of Sciences*, 111(41), 14782–14787.
- Jiang, X., Tang, P. C., Chen, Q., Zhang, X., Fan, Y. Y., Yu, B. C., ... Zhang, X. L. (2019). Cordycepin Exerts Neuroprotective Effects via an Anti-Apoptotic Mechanism based on the Mitochondrial Pathway in a Rotenone-Induced Parkinsonism Rat Model. *CNS & Neurological Disorders - Drug Targets*, 18(8), 609–620.
- Kemp, C. M., & Parr, T. (2012). Advances in apoptotic mediated proteolysis in meat tenderisation. *Meat Science*, 92(3), 252–259.
- Lee, G. J., Chae, S. J., Jeong, J. H., Lee, S. R., Ha, S. J., Pak, Y. K., ... Park, H. K. (2011). Characterization of mitochondria isolated from normal and ischemic hearts in rats utilizing atomic force microscopy. *Micron*, 42(3), 299–304.
- Lee, G. J., Jeong, J. H., Lee, S., Choi, S., Pak, Y. K., Kim, W., & Park, H. K. (2013). Quantitative and qualitative analysis of heart mitochondria for evaluating the degree of myocardial injury utilizing atomic force microscopy. *Micron*, 44, 167–173.
- Lee, K. H., Ha, S. J., Woo, J. S., Lee, G. J., Lee, S. R., Kim, J. W., ... Kim, W. (2017). Exenatide Prevents Morphological and Structural Changes of Mitochondria Following Ischaemia-Reperfusion Injury. *Heart, Lung, and Circulation*, 26(5), 519–523.
- Li, R., Luo, R. M., Luo, Y. L., Hou, Y. R., Wang, J. X., Zhang, Q., ... Zhou, J. L. (2022). Biological function, mediate cell death pathway and their potential regulated mechanisms for post-mortem muscle tenderization of PARP1: A review. *Frontiers in Nutrition*, 9, 1093939.
- Liu, C. M., Wei, Q. C., Li, X., Han, D., Liu, J. Q., Huang, F., & Zhang, C. H. (2022). Proteomic analyses of mitochondrial damage in postmortem beef muscles. *Journal of the Science of Food and Agriculture*, 102(10), 4182–4191.
- Liu, K., Shu, D., Song, N., Gai, Z., Yuan, Y., Li, J., ... Hong, H. (2012). The Role of Cytochrome c on apoptosis Induced by Anagrapha falcifera Multiple Nuclear Polyhedrosis Virus in Insect Spodoptera litura Cells. *PLoS One*, 7(8), e40877.
- Mukherjee, I., Ghosh, M., & Meinecke, M. (2021). MICOS and the mitochondrial inner membrane morphology - when things get out of shape. *FEBS Letters*, 595(8), 1159–1183.
- Pernas, L., & Scorrano, L. (2016). Mito-Morphosis: Mitochondrial Fusion, Fission, and Cristae Remodeling as Key Mediators of Cellular Function. *Annual Review of Physiology*, 78(1), 505–531.
- Quintana-Cabrera, R., Mehrotra, A., Rigoni, G., & Soriano, M. E. (2018). Who and how in the regulation of mitochondrial cristae shape and function. *Biochemical and Biophysical Research Communications*, 500(1), 94–101.
- Sun, M. G., Williams, J., Munoz-Pinedo, C., Perkins, G. A., Brown, J. M., Ellisman, M. H., ... Frey, T. G. (2007). Correlated three-dimensional light and electron microscopy reveals transformation of mitochondria during apoptosis. *Nature Cell Biology*, 9(9), 1057–1065.
- Ulivieri, C. (2010). Cell death: Insights into the ultrastructure of mitochondria. *Tissue and Cell*, 42(6), 339–347.
- Wang, L. L., Han, L., Ma, X. L., Yu, Q. L., & Zhao, S. N. (2017). Effect of mitochondrial apoptotic activation through the mitochondrial membrane permeability transition pore on yak meat tenderness during postmortem aging. *Food Chemistry*, 234, 323–331.
- Wang, L. L., Yu, Q. L., Han, L., Ma, X. L., Song, R. D., Zhao, S. N., & Zhang, W. H. (2018). Study on the effect of reactive oxygen species-mediated oxidative stress on the activation of mitochondrial apoptosis and the tenderness of yak meat. *Food Chemistry*, 244, 394–402.
- Zhang, J., Ma, D., & Kim, Y. H. B. (2020). Mitochondrial apoptosis and proteolytic changes of myofibrillar proteins in two different pork muscles during aging. *Food Chemistry*, 319, Article 126571.
- Zhang, J., Ma, G., Guo, Z., Yu, Q., Han, L., Han, M., & Zhu, Y. (2018). Study on the apoptosis mediated by apoptosis-inducing-factor and influencing factors of bovine muscle during postmortem aging. *Food Chemistry*, 266, 359–367.